

# Chip-to-chip optical interconnect using gold long-range surface plasmon polariton waveguides

Jin Tae Kim<sup>1,2\*</sup>, Jung Jin Ju<sup>1\*\*</sup>, Suntak Park<sup>1</sup>, Min-su Kim<sup>1</sup>, Seung Koo Park<sup>1</sup>, and Myung-Hyun Lee<sup>3</sup>

<sup>1</sup> Convergence Components and Materials Research Laboratory, ETRI, Daejeon 305-700, Korea

<sup>2</sup> School of Electrical Engineering and Computer Science, KAIST, Daejeon 305-701, Korea

<sup>3</sup> School of Information and Communication Engineering, Sungkyunkwan University, Suwon 440-746, Korea

\*E-mail address: [jintae@etri.re.kr](mailto:jintae@etri.re.kr)

\*\*Corresponding author: [jjju@etri.re.kr](mailto:jjju@etri.re.kr)

**Abstract:** We demonstrate a novel on-board chip-to-chip optical interconnect using long-range surface plasmon polariton (LR-SPP) waveguides that feature 2.5-cm-long gold strips embedded in a low loss polymer cladding. A TM-mode vertical-cavity surface-emitting laser (VCSEL) operating at a wavelength of 1.3  $\mu\text{m}$  was butt-coupled into the waveguides in order to excite a fundamental LR-SPP mode and then the transmitted light was received with a photo-diode (PD). The waveguide width is varied in the range of 1.5-5.0  $\mu\text{m}$  in order to optimize the insertion loss where the 3- $\mu\text{m}$ -wide waveguide provides a minimum insertion loss of -17 dB, consisting of 6 dB/cm propagation loss and 2 dB coupling loss. An interconnect system based on the optimized waveguide with a 4-channel array is assembled with the arrayed optoelectronic chips. It shows the feasibility of 10 Gbps (2.5 Gbps  $\times$  4 channels) signal transmission indicating that the LR-SPP waveguide is a potential transmission line for optical interconnection.

©2008 Optical Society of America

**OCIS codes:** (200.4650) Optical interconnects; (240.6680) Surface plasmons; (130.3120) Integrated optics devices.

---

## References and links

1. P. Berini, "Plasmon-polariton waves guided by thin lossy metal films of finite width: Bound modes of symmetric structures," *Phys. Rev. B* **61**, 10484-10503 (2000).
2. T. Nikolajsen, K. Leosson, I. Salakhutdinov, and S. I. Bozhevolnyi, "Polymer-based surface-plasmon-polariton stripe waveguides at telecommunication wavelengths," *Appl. Phys. Lett.* **82**, 668 (2003).
3. R. Charbonneau, C. Scales, I. Breukelaar, S. Fafard, N. Lahoud, G. Mattiussi, P. Berini, "Passive integrated optics elements based on long-range surface plasmon polaritons," *J. Lightw. Technol.* **24**, 477-494 (2006).
4. A. Boltasseva and S. I. Bozhevolnyi, "Directional couplers using long-range surface plasmon polariton waveguides," *IEEE J. Sel. Topic. Quantum. Electron.* **12**, 1233-1241 (2006).
5. T. Nikolajsen, K. Leosson, and S. I. Bozhevolnyi, "Surface plasmon polariton based modulators and switches operating at telecom wavelengths," *Appl. Phys. Lett.* **88**, 5833-5835 (2004).
6. S. Jetté-Charbonneau, P. Berini, "External cavity laser using a long-range surface plasmon grating as a distributed Bragg reflector," *Appl. Phys. Lett.* **91**, 181114 (2007).
7. J. T. Kim, S. Park, J. J. Ju, S. K. Park, M.-s. Kim, and M.-H. Lee, "Low-loss polymer-based long-range surface plasmon-polariton waveguide," *IEEE Photon. Technol. Lett.* **19**, 1374-1376 (2007).
8. S. Park, M.-s. Kim, J. T. Kim, S. K. Park, J. J. Ju, and M.-H. Lee, "Long range surface plasmon polariton waveguides at 1.31 and 1.55  $\mu\text{m}$  wavelengths," *Opt. Commun.* **281**, 2057-2061 (2008).
9. J. J. Ju, M.-s. Kim, S. Park, J. T. Kim, S. K. Park, and M.-H. Lee, "10 Gbps optical signal transmission via long-range surface plasmon polariton waveguide," *ETRI J.* **29**, 808-810 (2007).
10. J. J. Ju, S. Park, M.-s. Kim, J. T. Kim, S. K. Park, Y. J. Park, and M.-H. Lee, "40 Gbit/s light signal transmission in long-range surface plasmon waveguides," *Appl. Phys. Lett.* **91**, 171117 (2007).
11. P. Berini, "Long-range surface plasmon-polariton waveguides in silica," *J. Appl. Phys.* **102**, 053105 (2007).

## 1. Introduction

Since low loss lightwave guidance along a thin metal strip embedded in a dielectric material was explained theoretically by the long-range surface plasmon polariton (LR-SPP) [1], LR-SPP-based optical waveguides have attracted great attention in integrated optical devices and numerous optical components have been investigated [2-6].

Of these, polymer-based LR-SPP waveguides whose metal strips are embedded in low-loss polymer cladding material demonstrate that propagation loss can be reduced to 2.0 dB/cm and 1.4 dB/cm at the telecommunication wavelengths of 1.3  $\mu\text{m}$  and 1.5  $\mu\text{m}$ , respectively, and that light coupling efficiency with standard single-mode optical fiber can be reduced to 0.5 dB [7, 8]. In addition, pig-tailed polymer-based LR-SPP waveguides demonstrate their ability to transmit a high bit-rate optical signal of 40 Gbps [9, 10]. Thus, the polymer-based LR-SPP waveguide is considered a new optical wave guiding medium, replacing the conventional dielectric optical waveguide in parallel chip-to-chip optical interconnects.

This research focuses on the practical implementation of LR-SPP waveguides in on-board chip-to-chip optical interconnect systems. To demonstrate short-distance optical data communication, an Au LR-SPP waveguide is directly butt-coupled with a vertical-cavity surface-emitting laser (VCSEL) and a photodiode (PD). In order to excite the fundamental LR-SPP mode, the light from the VCSEL is TM-polarized. The optical properties of the LR-SPP waveguide when it is coupled to optoelectronic devices are investigated at a wavelength of 1.3  $\mu\text{m}$ . We have performed a 2.5 Gbps optical signal transmission experiment for four waveguide channels.

## 2. Fabrication and experiment

In order to implement an on-board chip-to-chip optical interconnect using an LR-SPP waveguide, a simple chip-to-chip optical interconnect system supporting 10 Gbps (2.5 Gbps  $\times$  4 channels) was designed as shown in Fig. 1. It consists of an optical transmitter (Tx) module, a receiver (Rx) module, and a polymer-based LR-SPP waveguide. The Tx module comprises a driver IC and a VCSEL array chip. The receiver IC comprises a receiver IC and a photo-diode (PD) array chip.

Driver and receiver ICs from SiRES LABS were used for four channels of 2.5 Gbps signal processing. To ensure reliable and high-speed electrical interconnection of Tx/Rx modules, a differential-coupled micro-strip line with 100 ohm differential characteristic impedance is employed in the electric circuits.

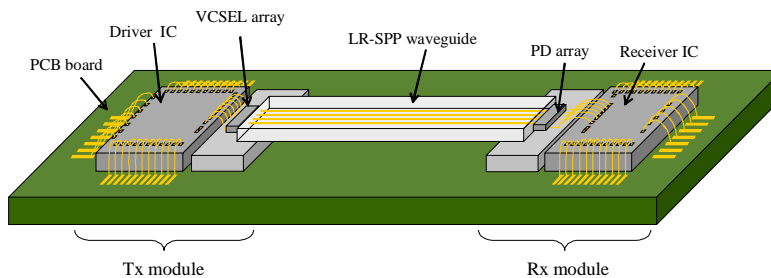


Fig. 1. Architectural view of on-board chip-to-chip optical interconnect using polymer-based Au long-range surface plasmon polariton (LR-SPP) waveguide.

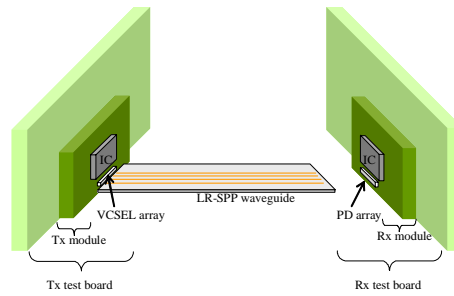


Fig. 2. Schematics of chip-to-chip optical interconnect transmission test set-up.

The polymer-based LR-SPP waveguide consists of a 14.5 nm-thick Au strip and a dielectric polymer cladding whose refractive index is 1.46 at a wavelength of 1.3  $\mu\text{m}$ . Detailed fabrication processes and optical properties such as the propagation loss and coupling loss with standard single-mode fiber (SMF) were described in our previous studies [7, 8].

The operation principle is as follows. An electrical signal from a pulse pattern generator (PPG) is transmitted to the driver IC through the differential line. Then, the electrical signal from the driver IC is transmitted to the VCSEL. A TM-polarized beam (1.3  $\mu\text{m}$  wavelength) from the VCSEL excites a fundamental LR-SPP wave, the  $SS_b^0$  mode [1], via a direct end-fire coupling. Subsequently, the wave propagates along the metal strip, and then the beam reaches the PD array. The electrical signal from the PD is magnified by the receiver IC consisting of a TIA and a limiting amp. Finally, the electrical signal is investigated with a digital communication analyzer (DCA).

To investigate the optical properties of the Au LR-SPP waveguide when it is coupled to the TM-polarized VCSEL, a simple chip-to-chip optical transmission testing assembly consisting of a Tx/Rx module, a Tx/Rx test board, and an LR-SPP waveguide was prepared, as shown in Fig. 2. One end of the 2.5 cm-long LR-SPP waveguide array was aligned with the VCSEL's aperture through direct butt-coupling without index matching liquid. Then the output face of the waveguide was imaged with a charge-coupled device (CCD). The captured mode profile was fitted with a Gaussian distribution to estimate the mode field diameter (MFD). After capturing the mode image, the transmitted powers were measured separately with an optical power meter through SMF to evaluate insertion loss. After maximum optical coupling was achieved with the SMF, the horizontal and vertical scanning of the VCSEL was carried out to estimate the 3 dB alignment tolerance. On the other hand, measurement of the PD's 3 dB tolerance to the metal waveguide was not performed because the PD has a large enough receiving area of 50  $\mu\text{m}$  (in diameter).

Figure 3 shows the MFDs and the insertion loss with the TM-polarized VCSEL as a function of metal strip width at the fixed Au thickness of 14.5 nm. Similar experimental results were observed; that is, the horizontal and vertical MFDs became broader as the metal width narrowed. Compared to the MFDs excited with 1.55  $\mu\text{m}$  wavelength light [8], the MFDs measured with 1.3  $\mu\text{m}$  light source showed a smaller value. As predicted by theory [1], the fundamental LR-SPP mode is more tightly confined at shorter wavelengths for a given metal geometry, resulting in a narrower MFD and higher absorption.

The measured insertion loss first decreases and then increases according to the increment of the metal strip width. These results show a similar pattern to that of the values obtained with SMF. Although the narrower metal strip waveguide has comparatively lower propagation loss, the increasing insertion loss in the region of the strip widths smaller than 3  $\mu\text{m}$  mainly result from the large coupling loss due to the mode field mismatch between the LR-SPP wave and the VCSEL mode (the MFD  $\sim$  10  $\mu\text{m}$ ). As shown in Fig. 3, the horizontal MFD is larger than the vertical one, and their differences are increased as the metal width decreases. Therefore, the MFD mismatch between the light source and the metal waveguide increases as the metal width decreases. On the other hand, the insertion loss of the metal widths larger than

3  $\mu\text{m}$  is mainly influenced by the propagation loss since the variation of the coupling loss in the region of the 3.0 ~ 5.0  $\mu\text{m}$  strip widths is relatively small. As previous studies showed, the coupling loss of the Au LR-SPP to SMF can be reduced to a value of 0.5 dB/facet [7, 8]. However, the propagation loss increases dramatically with the increment of the metal width. As a result, the insertion loss of wider metal width increases. The lowest insertion loss was achieved at the 3  $\mu\text{m}$  metal width.

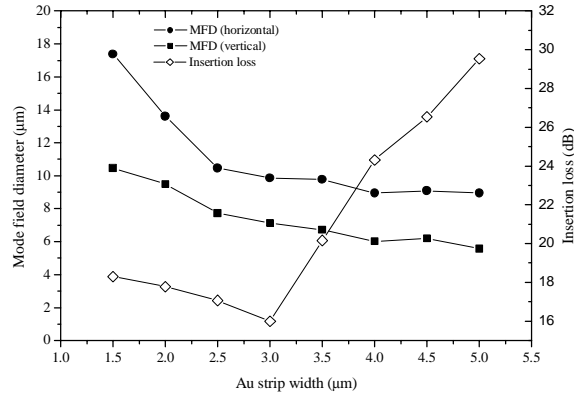


Fig. 3. Mode field diameter and insertion loss as functions of metal strip width. Values are measured at 1.3  $\mu\text{m}$  wavelength.

Figure 4 shows horizontal and vertical 3 dB alignment tolerances of the Au LR-SPP waveguide with the TM-polarized VCSEL in relation to the metal strip width. From the optical power variation measured under horizontal and vertical VCSEL scanning, a coupling tolerance of 3 dB was estimated. As expected from the MFD measurement, the estimated values increase as the metal width narrows. In particular, the horizontal 3 dB coupling tolerances are slightly larger compared to those of the vertical direction, and the difference between them increases as the metal strip width narrows. The largest horizontal and vertical 3 dB alignment tolerances were measured to be  $\pm 7 \mu\text{m}$  and  $\pm 5.2 \mu\text{m}$ , respectively, for the strip width of 1.5  $\mu\text{m}$ .

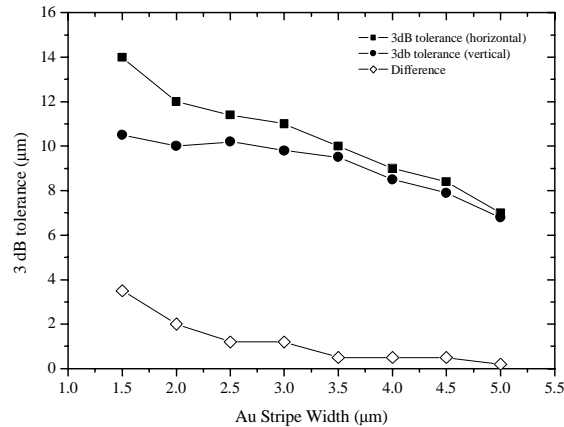


Fig. 4. Horizontal and vertical 3 dB alignment tolerances of the Au LR-SPP with the TM-polarized VCSEL in relation to the metal strip width.

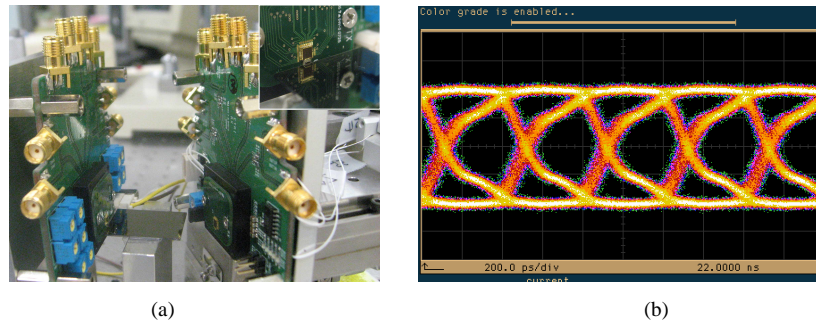


Fig. 5. (a). Assembled chip-to-chip optical interconnect system using the Au LR-SPP waveguide (the inset shows the coupling between the TM-polarized VCSEL and the Au LR-SPP waveguide), and (b) measured optical eye diagram for one channel (2.5 Gbps data rate) of the four receiver channels.

Although the lower propagation loss of the narrower metal strip width is advantageous for chip-to-chip optical interconnects, the higher coupling loss between the TM-polarized VCSEL and the Au LR-SPP waveguide is disadvantageous. Thus, we have to optimize the trade-off between propagation loss and coupling loss when the Au LR-SPP waveguide is used for chip-to-chip optical interconnects. Considering the insertion loss and a power budget of 20 dB, a 3  $\mu\text{m}$  wide LR-SPP waveguide was chosen for our practical chip-to-chip optical signal transmission experiment.

To implement the chip-to-chip optical interconnect experiment, one end of the Au LR-SPP waveguide array was aligned into the VCSEL's aperture, and a current indicator in the receiver IC was used to monitor the degree of alignment between the waveguide output and the PD. The average insertion loss was -17 dB, which is the sum of 6 dB/cm times 2.5 (the waveguide length in cm unit) for the propagation loss and 2 dB for the coupling loss. Since index matching liquid was not used between the metal waveguide and the optoelectronic devices, the insertion loss can be reduced if the liquid is used.

Figure 5(a) shows the assembled chip-to-chip optical interconnect test system installed with the polymer-based Au LR-SPP waveguide, and Fig. 5(b) shows the measured eye diagram for one channel of the receiver module. A 2.5 Gbps non-return-to-zero pseudorandom bit sequence ( $2^{23}-1$ ) of the optical signals was transmitted through the metal waveguide. The eye diagram for one optimized channel was clearly open at room temperature. The peak-to-peak timing jitter was 132 ps, and the rise and fall times for the received waveform were 250 ps and 300 ps, respectively. The bit error rate (BER) obtained under the best condition was estimated to  $10^{-10}$ .

For better BER and error-free transmission of optical signal, the optical power reaching the PD should be increased. This requirement can be achieved by minimizing the insertion loss of the polymer-based Au LR-SPP waveguide. Using low-loss polymer materials having a low refractive index and absorption loss at a telecom wavelength can improve the optical properties of the LR-SPP waveguide [7]. Substitution of Au by Ag is another suggestion to reduce the propagation loss of the LR-SPP waveguides since Ag has lower mode propagation attenuation (MPA) than that of Au [11].

On the other hand, the eye diagram in Fig. 5(b) shows the influence of all components because the pseudo random electrical bits pass through a long pathway, including the SMA connector, the Tx test board, the connector between board and module, the Tx module consisting of the VCSEL driver IC and the VCSEL, the Au LR-SPP waveguide, and reversed path components from the PD to SMA connectors. Therefore, the BER could be improved by simplifying the electric signal pathway.

### **3. Conclusion**

To configure an on-board chip-to-chip optical interconnect using an Au LR-SPP waveguide, a polymer-based Au LR-SPP waveguide was developed and its optical characteristics with optoelectronic devices, including a TM-polarized VCSEL and a PD were investigated. With a simple Tx/Rx module supporting direct end-fire coupling between the Au LR-SPP waveguide and the optoelectronic chips, 10 Gbps (four channels of 2.5Gbps) data transmission was successfully accomplished at a wavelength of 1.3  $\mu\text{m}$ . These results show that the polymer-based Au LR-SPP optical waveguide is a potential transmission line for very short-range direct chip-to-chip optical interconnects.

### **Acknowledgments**

The authors would like to express their gratitude to Professor Sang-Yung Shin of KAIST for valuable discussions. This work was supported by the IT R&D program [2006-S-073-02] of the MKE/IITA, Korea.